Supplement to *Divide migration and escarpment retreat: numerical models and application to the rift margin of Madagascar*

Yanyan Wang[1]; Sean D. Willett[1]; Datian Wu[2]

[1]ETH Zurich, Department of Earth Sciences, Sonneggstrasse 5, 8092 Zurich, Switzerland.

[2]China Geological Survey, Shengyang Center, Huanghe North Street 280, 110034 Shenyang, China.

Corresponding author: Yanyan Wang (yanyan.wang@erdw.ethz.ch)

Supplement includes:

- Five supplementary figures
- Four supplement tables
- Five supplement movies

Supplement figures:

- Figure S1 Chemical index of alteration (CIA) from river sediment of Madagascar.
- Figure S2 Plagioclase index of alteration (PIA) from river sediment of Madagascar.
- Figure S3 Weathering index of Parker (WIP) from river sediment of Madagascar.
- Figure S4 Escarpment river types of the southern Western Ghats in India.
- Figure S5 Regressions including rock erodibility of Madagascar and the Western Ghats, India.

Supplement tables:

- Table S1 Fixed default simulation parameters of simulations S0-S1 and S20-S23.
- Table S2 Varying simulation parameters of simulations S0-S1 and S20-S23.
- Table S3 Identical default simulation parameters of simulations S2 to S19.
- Table S4 Varying simulation parameters of simulations S2 to S19.

Supplement movies:

- Movie S1 Model behavior of the homogenous substrate model.
- Movie S2 Model behavior of the weak surface layer model.
- Movie S3 Comparison of a homogenous substrate and weak surface layer models.
- Movie S4 Comparison of the homogenous substrate model with different heights.
- Movie S5 Comparison of the weak surface layer with different heights.

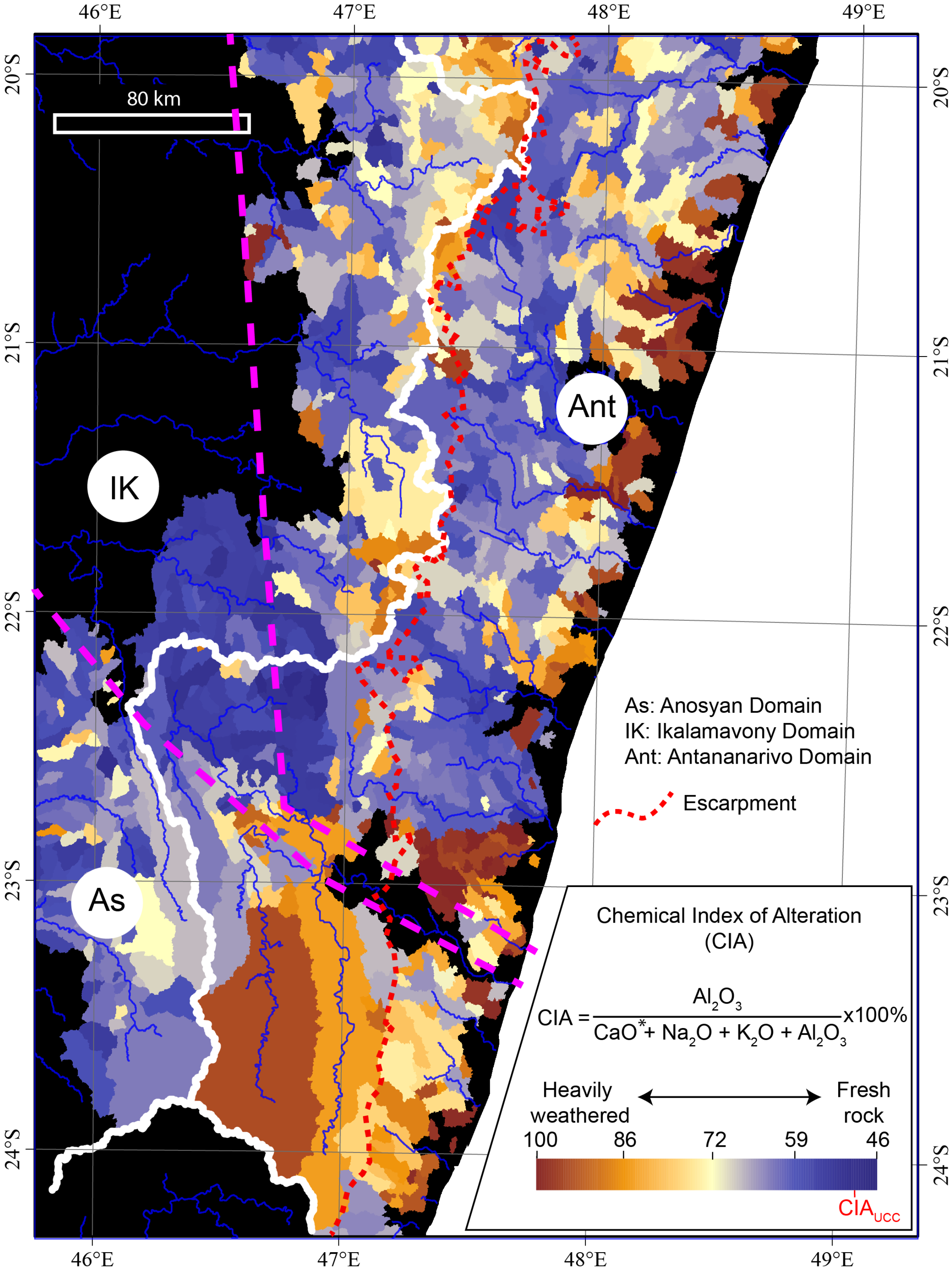

Fig. S1 Chemical index of alteration (CIA, Nesbitt and Young, 1982) from river sediment of Madagascar. High CIA indicates a high degree of weathering. The mean CIA of average elemental compositions of upper continental crust (CIA_{UCC}) is from Rudnick and Gao (2005). The three geological domains (As, IK, and Ant) are indicated and are different in age and major lithological composition (Tucker et al., 2014). Compositional and morphological effects are evident with low CIA in the IK and on the escarpment. Higher values of CIA are observed on both the plateau and the coastal lowlands.

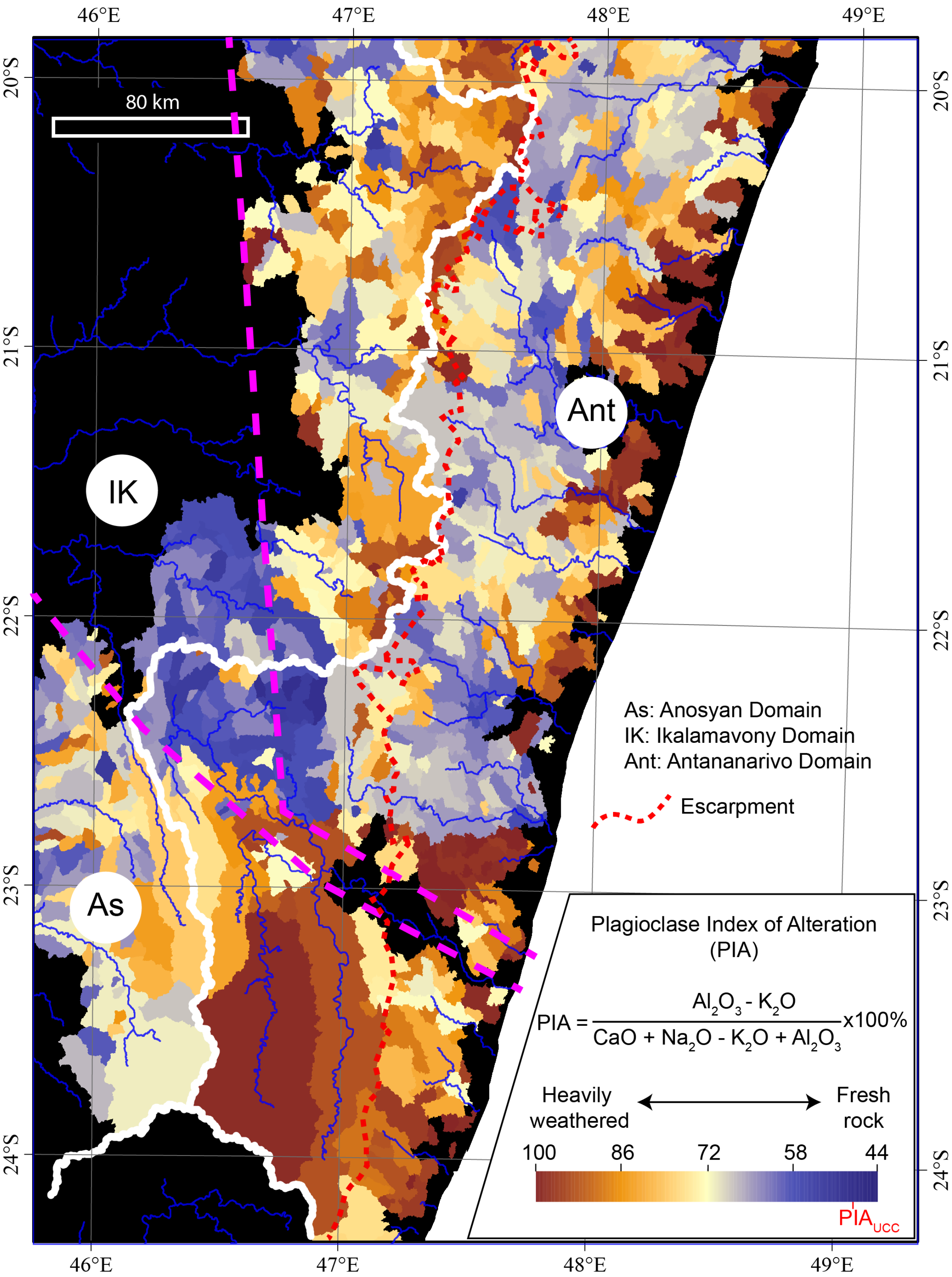

Fig. S2 Plagioclase index of alteration (PIA, Fedo et al., 1995) from river sediment of Madagascar. High PIA indicates a high degree of weathering. The mean PIA of average elemental compositions of upper continental crust (PIA_{UCC}) is from Rudnick and Gao (2005). The three geological domains (As, IK, and Ant) are indicated and are different in age and major lithological composition (Tucker et al., 2014). Compositional and morphological effects are evident with low PIA in the IK and on the escarpment. Higher values of PIA are observed on both the plateau and the coastal lowlands.

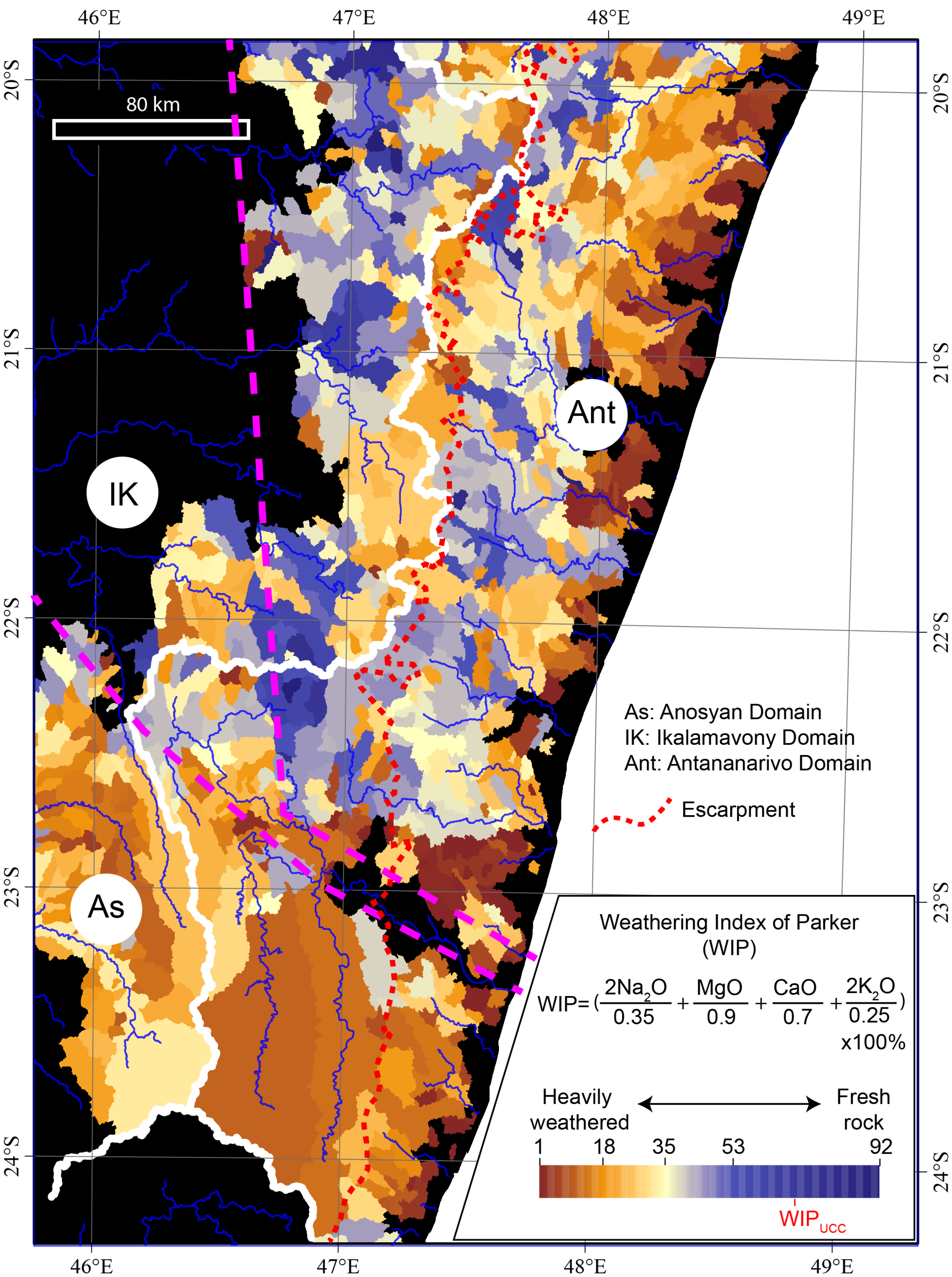

Fig. S3 Weathering index of Parker (WIP, Lecomte, 2014) from river sediment of Madagascar. Low WIP indicates a high degree of weathering. The mean WIP of average elemental compositions of upper continental crust (WIP_{UCC}) is from Rudnick and Gao (2005). The three geological domains (As, IK, and Ant) are indicated and are different in age and major lithological composition (Tucker et al., 2014). Compositional and morphological effects are evident with high WIP in the IK and on the escarpment. Lower values of WIP are observed on both the plateau and the coastal lowlands.

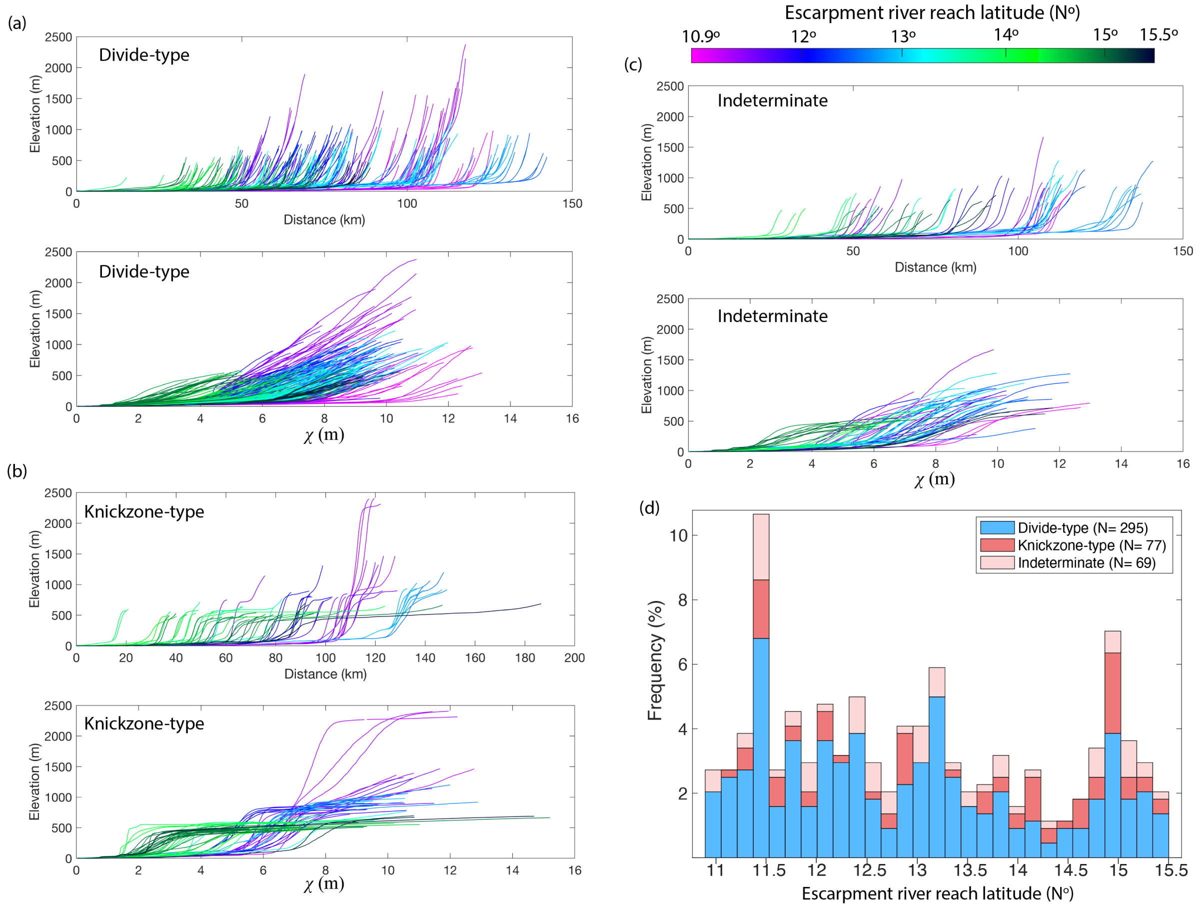

Fig. S4 Escarpment river types of the southern Western Ghats in India where the escarpment develops on the Precambrian basement. (a) Escarpment river profiles exhibiting divide-type, plotted against distance and normalized distance (Perron and Royden, 2013) and colored by the latitude of channel head. (b) Escarpment river profiles exhibiting knickzone-type, plotted in the same manner as (a). (c) Escarpment river profiles of indeterminate form, plotted in the same manner as (a). (d) Spatial variation of escarpment river type along the strike of the great escarpment. The number of escarpment river reaches is shown in the key.

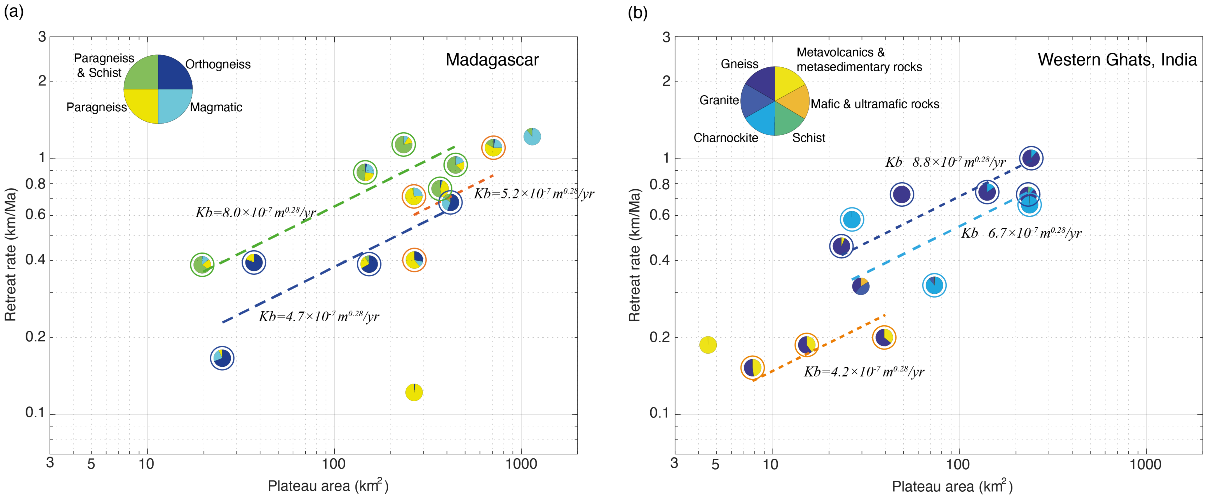

Fig. S5 Regressions of retreat rate, subdivided by substrate type of (a) Madagascar escarpment, (b) Escarpment-draining basins of Western Ghats, India. Each pie chart represents an escarpment basin. The pie chart shows the relative percentage of different rock types. The erodibility of major rock types is calculated by fitting a power exponent of the drainage area of 0.36. Basins used for erodibility calculation are indicated with open circles, colored consistent with the fit (dashed lines). The rock type of Madagascar escarpment is taken from the geological map of Madagascar (Roig et al., 2012). The rock type of Western Ghats escarpment-draining basins is from (Mandal et al., 2015).

Table S1 Fixed default parameters of simulations S0-S1 and S20-S23.

<table>
<tr><td rowspan="11">Simulation 0-1 and 20-23</td><td>Default parameters</td><td>Symbol</td><td>Value</td></tr>
<tr><td>Stream power law slope exponent</td><td>n</td><td>1</td></tr>
<tr><td>Stream power law discharge exponent</td><td>m</td><td>0.495</td></tr>
<tr><td>Inverse Hack's law power</td><td>H</td><td>2</td></tr>
<tr><td>Inverse Hack's law coefficient</td><td>k_a</td><td>1.66667</td></tr>
<tr><td>Critical hillslope length</td><td>X_c</td><td>1000 m</td></tr>
<tr><td>Critical hillslope angle</td><td>θ</td><td>21 degree</td></tr>
<tr><td>Hillslope diffusivity</td><td>K_f</td><td>0.14 m^2/yr</td></tr>
<tr><td>Substrate erodibility</td><td>K_b</td><td>0.000005 $m^{0.2}$/yr</td></tr>
<tr><td>Precipitation rate</td><td>p</td><td>1 m/yr</td></tr>
<tr><td>Uniform isostatic uplift rate</td><td>U</td><td>0.000005 m/yr</td></tr>
</table>

Table S2 Varying parameters of simulations S0-S1 and S20-S23.

Simulation number	Plateau height (Z_p, m)	Regolith thickness (T_{hw}, m)	Erodibility ratio (K_w/K_b)
0	2600	0	1
1	2600	10	100
20	3200	10	100
21	3800	10	100
22	4400	10	100
23	5000	10	100

Table S3 Fixed default parameters of simulations S2 to S19.

	Default parameters	Symbol	Value
Simulation 2-19	Stream power law slope exponent	n	1
	Stream power law discharge exponent	m	0.4
	Inverse Hack's law power	H	1.667
	Inverse Hack's law coefficient	k_a	6.7
	Critical hillslope length	X_c	295 m
	Critical hillslope angle	θ	21 degree
	Hillslope diffusivity	K_f	0.14 m^2/yr
	Substrate erodibility	K_b	0.000005 $m^{0.2}$/yr
	Precipitation rate	p	1 m/yr
	Uniform isostatic uplift rate	U	0.000005 m/yr

Table S4 Varying parameters of simulations S2 to S19.

Simulation number	Plateau height (Z_p, m)	Regolith thickness (T_{hw}, m)	Erodibility ratio (K_w/K_b)
2	500	0	1
3	1000	0	1
4	2000	0	1
5	3000	0	1
6	4000	0	1
7	5000	0	1
8	6000	0	1
9	1000	15	100
10	1000	15	200
11	1000	15	300
12	1000	15	50
13	1000	15	30
14	1000	15	10
15	1000	5	50
16	1000	10	50
17	1000	20	50
18	1000	25	50
19	1000	30	50

References

Fedo, C.M., Nesbitt, H.W., Young, G.M., 1995. Unraveling the effects of potassium metasomatism in sedimentary rocks and paleosols, with implications for paleoweathering conditions and provenance. Geology 23, 921–924.

Lecomte, P.J.D.A.I.P.K.L., 2014. Weathering and the Riverine Denudation of Continents, SpringerBriefs in Earth System Sciences. https://doi.org/10.1007/978-94-007-7717-0

Mandal, S.K., Lupker, M., Burg, J.P., Valla, P.G., Haghipour, N., Christl, M., 2015. Spatial variability of 10Be-derived erosion rates across the southern Peninsular Indian escarpment: A key to landscape evolution across passive margins. Earth and Planetary Science Letters 425, 154–167. https://doi.org/10.1016/j.epsl.2015.05.050

Nesbitt, Hw., Young, G.M., 1982. Early Proterozoic climates and plate motions inferred from major element chemistry of lutites. nature 299, 715–717.

Perron, J.T., Royden, L., 2013. An integral approach to bedrock river profile analysis. Earth Surface Processes and Landforms 38, 570–576. https://doi.org/10.1002/esp.3302

Roig, J.Y., Tucker, R.D., Peters, S.G., Delor, C., Theveniaut, H., 2012. Carte Géologique de la République de Madagascar à 1/1,000,000, Ministère des Mines, Direction de la Géologie, Programme de Gouvernance des Resources Minérales.

Rudnick, R.L., Gao, S., 2005. Composition of the Continental Crust, in: Rudnick, R.L. (Ed.), The Crust.

Tucker, R.D., Roig, J.Y., Moine, B., Delor, C., Peters, S.G., 2014. A geological synthesis of the Precambrian shield in Madagascar. Journal of African Earth Sciences 94, 9–30. https://doi.org/10.1016/j.jafrearsci.2014.02.001